Available online at www.sciencedirect.com
ScienceDirect
Polymer 49 (2008) 1266–1275
polymer
www.elsevier.com/locate/polymer

Electrospun cellulose acetate fibers containing chlorhexidine as a bactericide

Liang Chen, Lev Bromberg, T. Alan Hatton*, Gregory C. Rutledge*

Department of Chemical Engineering, Massachusetts Institute of Technology, 77 Massachusetts Avenue, Cambridge, MA 02139, USA

Received 19 November 2007; received in revised form 21 December 2007; accepted 5 January 2008
Available online 11 January 2008

Abstract

Submicron fibers with bactericidal properties were prepared from electrospinning of blends containing cellulose acetate (CA) as a polymer base, chlorhexidine (CHX) as a bactericidal agent, and organic titanate Tyzor® TE (TTE) as a cross-linker. A small amount of high molecular weight poly(ethylene oxide) (PEO) was incorporated into the blends to facilitate the electrospinning, and its effect on the extensional properties and spinnability of the *N*,*N*-dimethylformamide (DMF) solutions were evaluated. The CHX-containing fiber meshes were cured by TTE in the presence of water vapor, which created covalent links between the CA and CHX. The immobilization of CHX on or within the fibers was confirmed by FTIR, Raman and XPS measurements. The resulting fiber meshes exhibited bactericidal properties on contact, due to the CHX immobilized on the fibers, and within a zone of inhibition (ZoI), due to the release of unbound CHX. The relationship of ZoI for the gram-negative *Escherichia coli* and the gram-positive *Staphylococcus epidermidis* to the amount of unbound CHX in the fibers is described by a simple diffusion model. The contact bactericidal capacity against both *E. coli* and *S. epidermidis* was assayed after complete removal of unbound CHX from the fibers. A post-spin treatment to attach CHX onto CA–PEO fibers via TTE linkers was also shown to be effective.

Keywords: Bactericide; Electrospinning; Fiber

1. Introduction

Adhesion and proliferation of bacteria on the surfaces of materials can induce severe health and environmental hazards [1]. Hence, there is a great demand for bactericidal, antiseptic, and bacteriostatic materials that can prevent attachment, proliferation and survival of microbes on the material surface. A broad range of antibacterial agents such as silver, quaternary ammonium groups, hydantoin compounds, and tetracycline antibiotics have been incorporated into or attached onto the surfaces of various materials such as textiles and medical devices [2–6].

Electrospinning is a simple and versatile method for fiber preparation, which employs electrostatic forces that stretch a polymer jet to generate continuous fibers with diameters ranging from micrometers down to several nanometers [7–14]. Electrospun fiber meshes possess remarkable features such as small fiber diameter, high specific surface area, high porosity, and low fabric weight. These unique properties have triggered a broad range of potential applications, including nanocomposites [15,16], scaffolds for tissue engineering [17], sensors [18], protective clothing and filtration membranes [19,20], magneto-responsive fibers [21], and superhydrophobic membranes [22,23].

Currently, protective clothing is typically multilayered and acts as an effective barrier by chemically or physically absorbing chemical or biological hazards on the surfaces of the fabrics [24]. Effective protection comes at the cost of undesirable heavy weight and heat burdens placed on the wearers. This motivates the development of new protective clothing systems. We have begun to develop reactive fibers capable of destroying toxic chemical or biological agents on contact [20]. The high specific surface area of electrospun fibers and

* Corresponding authors.
E-mail addresses: tahatton@mit.edu (T.A. Hatton), rutledge@mit.edu (G.C. Rutledge).

0032-3861/$ - see front matter © 2008 Elsevier Ltd. All rights reserved.
doi:10.1016/j.polymer.2008.01.003

the self-supporting nature of nonwoven meshes consisting of these fibers make them good substrates for attachment of functional compounds or biocides to generate reactive or bactericidal fibers that could be incorporated as reactive and/or antibacterial layer(s) into new protective fabrics. Furthermore, the high porosity and low weight of electrospun fiber membranes can substantially mitigate the weight and heat burdens while offering effective protection.

Silver nanoparticles have been incorporated into electrospun fibers and shown to exhibit good antimicrobial activity [25,26]. Recently, quaternized chitosan with quaternary ammonium groups was electrospun into fibers by blending with other polymers such as poly(vinyl alcohol) and demonstrated high antibacterial activity [27,28]. In this work, we report on electrospun fiber meshes containing the biocide chlorhexidine, incorporated within and/or bound onto the surfaces of the fibers to obtain bactericidal membranes, intended for use in protective fabrics or antibacterial filtration media. Chlorhexidine (CHX) (Scheme 1) has been widely used as an effective antibacterial agent in applications that range from common disinfectants to bactericidal agents in dentistry; this is largely due to its broad range of antimicrobial activities against bacteria and fungi, high killing rate and nontoxicity toward mammalian cells [29,30]. The commonly cited mechanism of action of CHX is that two symmetrically positioned chlorophenyl guanide groups can penetrate through the cellular wall of bacteria and irreversibly disrupt the bacterial membrane, thus killing the microorganism. In most materials that include CHX as the biocide, CHX is simply enmeshed within the material and gradually leaches out to kill the bacteria [31,32]. The disadvantage of such a loose association is that the antibacterial agent is eventually exhausted and the material has a limited functional life. In this work, dually functional antibacterial fibers were generated by electrospinning a series of blends of cellulose acetate (CA) and CHX with (a) a part of CHX bound to the CA polymer matrix by the organic titanate linker, Tyzor® TE (TTE), and (b) a significant fraction of CHX unbound but embedded within the fibers. Antibacterial CHX fibers were also produced by a post-spin treatment process to immobilize CHX on already prepared CA fibers. The resulting bactericidal electrospun CA–CHX fibers possessed significant antibacterial activity against both the gram-negative strain of *Escherichia coli* (*E. coli*) and the gram-positive strain of *Staphylococcus epidermidis* (*S. epidermidis*).

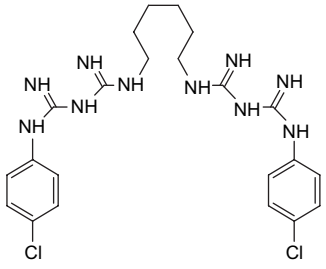

Scheme 1. Chlorhexidine (CHX).

2. Experimental

2.1. Materials

Cellulose acetate (CA) ($M_n = 50$ kDa), chlorhexidine (CHX) (98%), poly(ethylene oxide) (PEO) (viscosity-average molecular weight, $M_v = 2$ and 5 MDa), and *N*,*N*-dimethylformamide (DMF) were purchased from Sigma–Aldrich Chemical Co. (St. Louis, MO) and used as received. Tyzor® TE (TTE) (80 wt% titanium triethanolamine in isopropanol) was kindly supplied by DuPont de Nemours & Co. (Wilmington, DE) and used as received. Chlorhexidine digluconate aqueous solution (20% w/v) was purchased from Alfa Aesar Co. (Ward Hill, MA) and used as received. Bacteria *E. coli* and *S. epidermidis* were purchased from ATCC (Manassas, VA) and stored at −80 °C prior to use.

2.2. Polymer solution characterization and electrospinning

DMF is a good solvent for chlorhexidine powders as well as CA and thus was employed as the electrospinning medium in this work. The lack of elasticity of the CA solutions in DMF did not permit the formation of uniform fibers, however, and droplets were formed instead. A recent study by Yu et al. [33] demonstrated that the addition of a small amount of high molecular weight PEO into the spin solution can significantly increase the elasticity (extensional viscosity) of the solution and thus facilitate the electrospinning process. Following this approach, we incorporated relatively small amounts of PEO ($M_v = 2$ or 5 MDa) into the spin solutions in order to generate uniform fibers. A series of polymer solutions of 3 wt% CA with various concentrations of PEO in DMF were prepared. A capillary breakup extensional rheometer (CaBER 1; Thermo Electron Co.) was used to examine the extensional properties of the polymer solutions and relate these to the properties of the resulting fibers, to determine the concentration of PEO in polymer solutions required for the formation of uniform fibers.

CaBER is a filament stretching apparatus that measures the midpoint diameter, $D_{mid}(t)$, of the thinning filament over time when a fluid filament constrained axially between two coaxial disks is stretched rapidly over a short distance [34,35]. In these measurements, the Hencky strain, ε, and the apparent extensional viscosity, η_{app}, are related as follows [34]:

$$\varepsilon = 2\ln\left(\frac{D_0}{D_{mid}(t)}\right) \tag{1}$$

$$\eta_{app} = -\frac{\sigma}{dD_{mid}(t)/dt} \tag{2}$$

where D_0 is the initial diameter of the filament before stretching and σ is the surface tension of the fluid. The time evolution of $D_{mid}(t)$ for viscoelastic fluid is governed by a balance between surface tension and elasticity and can be described by the following model [35]:

$$D_{\mathrm{mid}}(t) = D_1\left(\frac{D_1 G}{4\sigma}\right)^{1/3} \mathrm{e}^{-t/3\lambda_p} \quad (3)$$

where D_1 is the initial midpoint diameter just after stretching, G is the elastic modulus, and λ_p is the fluid relaxation time, which is the characteristic time scale of viscoelastic stress growth.

A series of polymer solutions of 3 wt% CA, 0.2 wt% PEO ($M_v = 5$ MDa), 1 wt% TTE and various concentrations of CHX (0.3, 0.6, 0.9 and 1.2 wt%) were prepared by adding PEO, CA, chlorhexidine powders and TTE sequentially into DMF. The solutions were heated to 50 °C upon addition of PEO to facilitate the dissolution of the high molecular weight polymer. Then the polymer blends were stirred at room temperature until clear homogeneous solutions were obtained. The CHX-containing fibers produced from these solutions are denoted as CA–CHX fibers. Polymer solutions of 3 wt% CA, 0.2 wt% PEO ($M_v = 5$ MDa) and 1 wt% TTE without CHX were also prepared to produce nonfunctional cross-linked CA fibers, which are denoted as CA–TTE fibers. In addition, solutions of 3 wt% CA and 0.2 wt% PEO ($M_v = 5$ MDa) were prepared for post-spin treatment to attach CHX on the fiber surface. These fibers are denoted CA–PEO fibers.

An electrospinning apparatus similar to that described previously by Shin et al. [36] was used, except that the spun fibers were collected on a rotating drum ground electrode (3.5 cm in diameter, 20 cm in length and rotation rate of 250 rpm) instead of a plate collector, where the collected fibers discharged less efficiently and impeded accumulation of the fiber mesh. A syringe pump (Harvard Apparatus PHD 2000) was used to deliver polymer solution via a Teflon feedline to a capillary nozzle. Voltages up to 30 kV, generated by a power supply (Gamma High Voltage Research ES-30P), were applied between the upper plate and the ground drum to provide the driving force for electrospinning. The electrical potential, solution flow rate, and distance between the capillary nozzle and the collector were adjusted to 16–19 kV, 0.04 ml/min, and 45 cm, respectively, to obtain a stable jet.

2.3. CHX binding to the fibers

TTE is an organic titanate that has been applied as a cross-linking agent in adhesives, coatings, oil and gas products, and textiles [37,38]. It cross-links or binds compounds with hydroxyl, amino, amido, carboxyl and thio groups [6,37–39]. The cross-linking and titanate polymerization to form titania are activated at high temperature (100–250 °C) and/or in the presence of water [37]. We conducted control experiments to test the binding capability of TTE to CHX. The CHX powder and TTE solution were mixed at a weight ratio of 1:8 to form a yellowish homogeneous suspension. The suspension gradually became clear upon addition of a small amount of water due to the reaction of TTE with CHX, which facilitates the dissolution of CHX. Heating the solution to 70 °C accelerated the reaction process. The viscosity increased dramatically and the solution gradually became pink and pasty or gel-like in appearance, which is indicative of binding of TTE to CHX (Scheme 2).

In analogous experiments where binding between CHX and the CA polymer matrix via TTE linkers in the fiber meshes was desired, the fibers were placed in an environment of saturated water vapor at 70 °C for 4 days. The fibers turned slightly pink during the curing process, indicating the occurrence of a chemical reaction. A schematic of the binding chemistry (Scheme 2) depicts the reaction of the organic titanate TTE with the hydroxyl groups of CA and amino groups of CHX via transesterification reactions, to covalently bind CHX to the CA polymer matrix.

2.4. Quantification of CHX content in the fibers

Not all of the CHX molecules were covalently bound to the polymer matrix during the curing experiments. To determine the fraction of CHX that was not bound to the fibers, weighed fibers (10 mg) were placed in a sufficient quantity of water (100–200 ml) to ensure essentially complete release of free CHX. The unbound

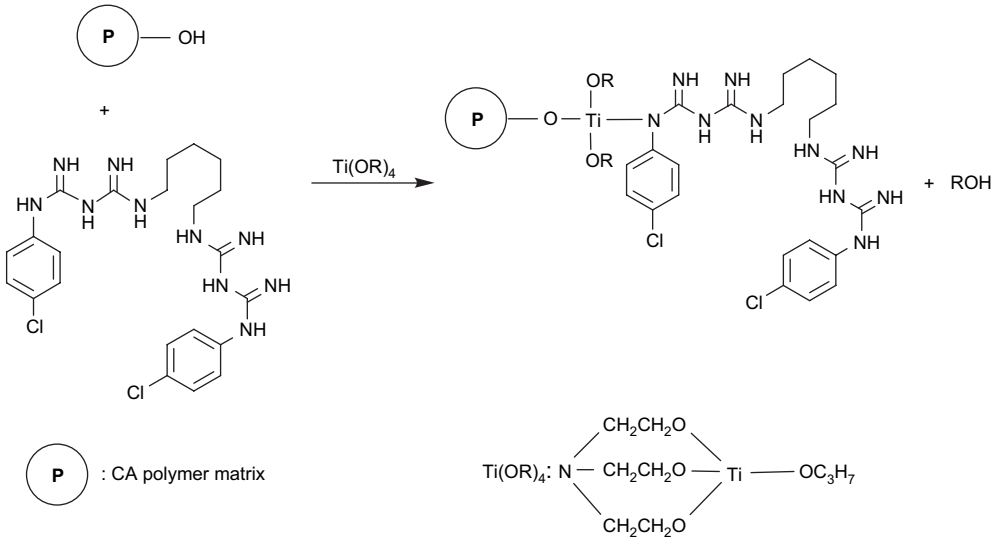

Scheme 2. Binding of amino groups of CHX to hydroxyl groups of the CA polymer matrix via titanate links using Tyzor® TE (TTE).

CHX that was gradually released upon immersion of the mesh in water was measured using a Hewlett–Packard 8453 UV–Vis spectrophotometer by monitoring a characteristic peak at 254 nm and using calibration (absorbance vs. CHX concentration) curves.

2.5. Fiber characterization

The fibers were examined by scanning electron microscopy (SEM) using a JEOL-6060 microscope (JEOL Ltd.) to visualize their morphology. A thin layer of gold (*ca.* 10 nm) was sputter-coated onto the fiber samples.

Prior to FTIR, Raman and XPS measurements, the cross-linked CA–CHX fiber meshes were placed in excess water for 12 h to remove completely the unbound CHX and dried under vacuum at room temperature to constant weight. The complete removal of the CHX not covalently linked to the fiber was ensured by monitoring the CHX concentration in the wash-outs. When no further removal of the CHX from the fibers into water was detected, the fibers were considered to be fully depleted of the unbound CHX.

FTIR spectra were measured in absorbance mode using a Nexus 870 spectrophotometer (Thermo Nicolet Co.) equipped with an ATR accessory. Two hundred and fifty-six scans were accumulated with a resolution of 4 cm^{-1}.

Raman spectra were measured with a Kaiser Hololab 5000R Raman spectrometer (Kaiser Optical Systems Inc.) with an excitation wavelength of 785 nm.

XPS measurements were carried out with a Krato Axis Ultra Imaging X-ray photoelectron spectrometer (Kratos Analytical Co.) equipped with a monochromatized Al Kα X-ray source.

2.6. Post-spin treatment of fibers

Bactericidal, CHX-containing CA–CHX fibers were also produced by post-spin treatment of CA–PEO fiber meshes. CA–PEO fibers were first electrospun from 3 wt% CA and 0.2 wt% PEO ($M_v = 5$ MDa) solutions in DMF. The CA–PEO fiber meshes thus formed were immersed for 1 h in 10 wt% titanium triethanolamine solution in isopropanol, which was obtained by dilution of the TTE solutions supplied by the manufacturer. The fiber meshes were cured at 110 °C for 10 min to bind TTE to CA. The fibers were then rinsed with water several times and dried. The resulting fibers were placed in 5% (w/v) chlorhexidine digluconate aqueous solution for 1 h and cured in the oven at 90 °C for 30 min to immobilize the CHX via the titanate linkers. The treated fibers were rinsed with water several times and dried under vacuum to constant weight. The applied temperatures were used as in Ref. [6], where organic titanates were successfully used to bind antibiotics onto cotton fabrics.

2.7. Antibacterial tests

2.7.1. Disk diffusion test

The release-killing capacity of unbound CHX in the CA–CHX fibers was determined by the disk diffusion test method. *E. coli* and *S. epidermidis* were cultured by adding 10 μl of the bacteria to 5 ml Luria–Bertani (LB) broth and incubating it under shaking at 37 °C overnight, followed by dilution with a phosphate buffer solution (PBS, pH 7.0) to approximately 5×10^6/ml. The bacteria were spread onto LB agar plates with cotton swabs. The round slide disks (diameter = 22 mm), to which the CA–CHX fibers were attached, were placed on top of the agar plates. The agar plates were inverted and incubated at 37 °C for 16–20 h. Duplicate experiments were conducted and the zone of inhibition (ZoI) was measured.

2.7.2. ASTM E2149-01 method

The CA–CHX fiber meshes were placed in excess water for 12 h to remove unbound CHX molecules, and dried under vacuum to constant weight. The contact-killing capacity of CA–CHX fibers was assayed according to a modified ASTM E2149-01 method (dynamic shake flask test) [40]. Briefly, *E. coli* and *S. epidermidis* were cultured overnight and diluted in PBS to approximately 10^6/ml. The fiber meshes (100 mg) were placed in a 50 ml bacterial suspension in a sterile flask and the suspension was shaken at 200 rpm at room temperature for 1 h using an orbital shaker. A certain amount of the suspension (100 μl) was retrieved from the flask before and after exposure to the mesh and plated with serial dilutions. After incubation of agar plates at 37 °C for 16–20 h, the number of viable colonies was counted visually and the reduction in the number of viable bacteria colonies was calculated after averaging the duplicate counts.

3. Results and discussion

3.1. Optimization of CA–PEO electrospinning process

Fig. 1(a) shows the time evolution of the midpoint diameter during the CaBER measurements for six CA–PEO polymer solutions consisting of 3 wt% CA with various concentrations of PEO ($M_v = 2$ and 5 MDa) ranging from 0.1 to 0.5 wt%. The filament breakup time increased with increasing PEO concentration, and was significantly higher for the higher (5 MDa) than for the lower (2 MDa) molecular weight PEO. The curves of apparent extensional viscosity vs. Hencky strain for these six solutions were derived from the time evolution data of midpoint diameter using Eqs. (1) and (2) and are shown in Fig. 1(b). A clear tendency toward extensional strain hardening was observed for these polymer solutions. The apparent extensional viscosity increased with the PEO concentration and molecular weight. A more elastic solution possesses a slower thinning rate and a longer breakup time due to the resistance to the capillary breakup during extensional deformation afforded by the elastic force. This accounts for the observed increase in the filament breakup time as PEO concentration and molecular weight were increased.

Fig. 2 shows the typical morphologies of the CA–PEO fibers electrospun from the above solutions. The lack of elasticity of the solutions with lower molecular weight and/or lower concentration of PEO leads to the formation of droplets (Fig. 2(a)). A transition in fiber morphology from a beads-on-string structure to a uniform fiber is observed with increasing PEO concentration and molecular weight (Fig. 2(b) and (c)). Uniform fibers are generated when the concentration of PEO

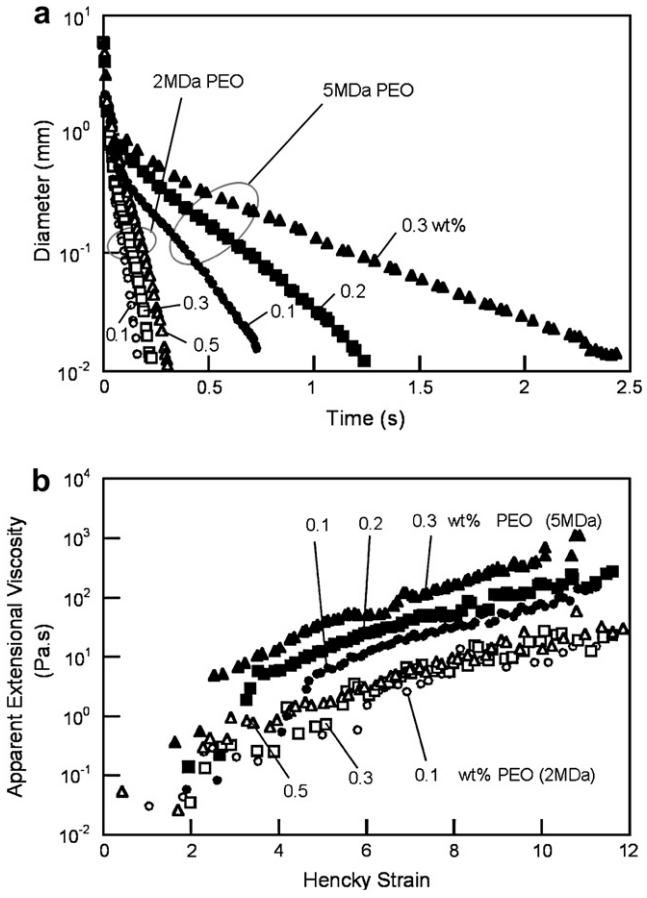

Fig. 1. Extensional properties of CA–PEO solutions: (a) filament diameter evolution curves; (b) extensional viscosity vs. Hencky strain.

($M_v = 5$ MDa) is at least 0.2 wt% at 3 wt% CA in DMF (Table 1). The relaxation times, λ_p, were obtained by fitting the elastic model described in Eq. (3) to the time evolution data of midpoint diameter in the range of exponential thinning. A dimensionless Deborah number, *De*, was introduced to examine the spinnability of the CA–PEO solutions. *De* is defined as the ratio of the fluid relaxation time, λ_p, to the Rayleigh instability growth time, t_R, as follows [35,41]:

$$De = \frac{\lambda_p}{t_R} \tag{4}$$

where

$$t_R = \frac{1}{\omega_{max}} = \sqrt{\frac{\rho R_0^3}{\sigma} \frac{I_0(x_R)}{I_1(x_R)(1-x_R^2)x_R}} \tag{5}$$

in which ω_{max} is the largest instability growth rate, σ is the surface tension, ρ is the density, R_0 is the initial radius of the polymer jet (0.8 mm in this work), x_R is the reduced wave number, and $I(x_R)$ is the modified Bessel function. Prior studies [42,43] have shown that viscoelasticity does not significantly affect the classical Rayleigh wavelength and only slightly increases the growth rate. Therefore, the classical Rayleigh instability growth rate for Newtonian fluids was used to estimate the instability growth time as shown in Eq. (5). The most unstable mode, corresponding to ω_{max}, occurs at $x_R = 0.697$. If the fluid relaxation time is much greater than the instability growth time ($De > 1$), the instability is fully suppressed or arrested by the viscoelastic response to produce uniform fibers. Table 1 summarizes the relaxation times, *De* numbers and fiber morphology of all the six tested CA–

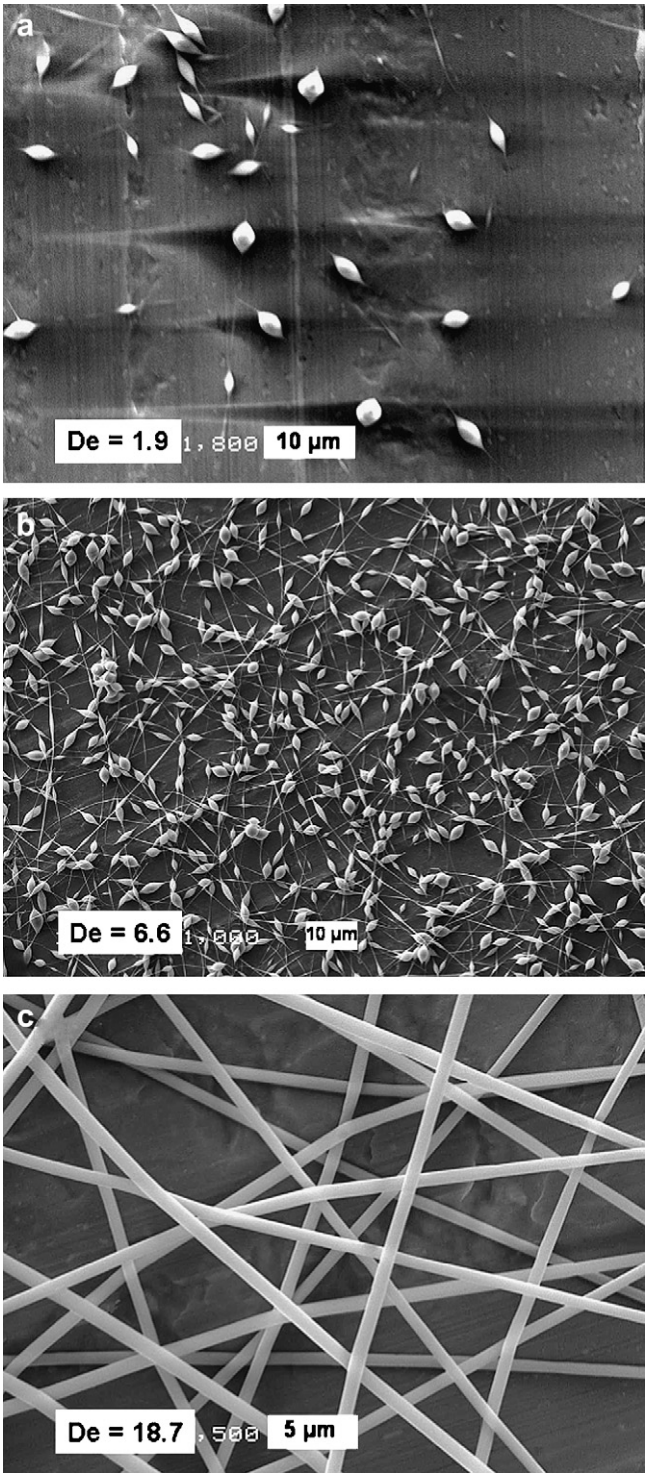

Fig. 2. Typical electrospun fiber morphologies for CA–PEO solutions: (a) 3 wt% CA, 0.3 wt% PEO (2 M), $De = 1.9$, droplets; (b) 3 wt% CA, 0.1 wt% PEO (5 M), $De = 6.6$, beads-on-string; (c) 3 wt% CA, 0.3 wt% PEO (5 M), $De = 18.7$, uniform fibers.

Table 1
Relaxation times, Deborah numbers and fiber morphology of CA–PEO solutions

Samples[a]	Relaxation time λ_p (s)	surface tension σ (mN/m)	*De*	Fiber morphology
0.1 wt% PEO (2 M)	0.013	35.6	1.2	No fibers
0.3 wt% PEO (2 M)	0.020	35.3	1.9	No fibers
0.5 wt% PEO (2 M)	0.021	35.0	2.0	Beads-on-string
0.1 wt% PEO (5 M)	0.072	34.1	6.6	Beads-on-string
0.2 wt% PEO (5 M)	0.105	34.4	9.6	Uniform fibers
0.3 wt% PEO (5 M)	0.201	35.6	18.7	Uniform fibers

[a] CA (3 wt%) in DMF.

PEO solutions. Only for $De > 7$ were uniform electrospun fibers produced, which is in accordance with the results on electrospun PEO/PEG fibers reported by Yu et al. [33]. Therefore, *De* is a good indicator of the spinnability of CA–PEO solutions. The addition of a small amount of high molecular weight PEO can increase the elasticity of polymer solutions and substantially facilitate the electrospinning of CA fibers.

3.2. Bactericidal CA–CHX fibers electrospun from polymer blends

3.2.1. Electrospinning

A series of solutions with 3 wt% CA, 0.2 wt% PEO, 1.0 wt% TTE and various concentrations of CHX (0.3, 0.6, 0.9 and 1.2 wt%) in DMF were electrospun successfully into fibers. The addition of CHX and coupling agent TTE did not impair the electrospinning process, and even facilitated it. The time evolution curves by CaBER measurements for these CHX-containing polymer solutions showed very similar or slightly smaller relaxation times compared to those of the CA–PEO solution without CHX and TTE (Table 2). However, the conductivity of polymer solutions was observed to increase upon the addition of TTE and CHX (Table 2), which is known to stabilize the electrospinning process [10,11]. Fig. 3(a) illustrates the typical morphology of electrospun CA–CHX fibers. There was no obvious change in fiber size as the concentration of CHX in the solutions was varied. The average size of these fibers was about 950 nm in diameter with the fiber sizes ranging from 700 to 1200 nm. A typical SEM image of fibers after curing is shown in Fig. 3(b). While the fiber size was not affected by the treatment, some fibers appeared to be coupled together at the junctions, and titanium clusters were observed to form on the surfaces of some fibers. The resultant CA–CHX fibers did not dissolve in THF, which indicated cross-linking of the fiber meshes by the organic titanate, while CA–PEO fibers produced without titanate dissolved in THF readily.

Table 2
Solution properties of polymer blends for electrospinning

Solutions[a]	Conductivity (μS/cm)	Relaxation time λ_p (s)	Surface tension σ (mN/m)
0 wt% TTE, 0 wt% CHX	0.23	0.105	35.6
1.0 wt% TTE, 0 wt% CHX	0.36	0.104	34.6
1.0 wt% TTE, 0.3 wt% CHX	0.92	0.101	34.3
1.0 wt% TTE, 0.6 wt% CHX	1.50	0.096	34.5
1.0 wt% TTE, 0.9 wt% CHX	1.23	0.092	33.9
1.0 wt% TTE, 1.2 wt% CHX	1.45	0.081	34.5

[a] CA (3 wt%) and 0.2 wt% PEO (5 M) in all solutions.

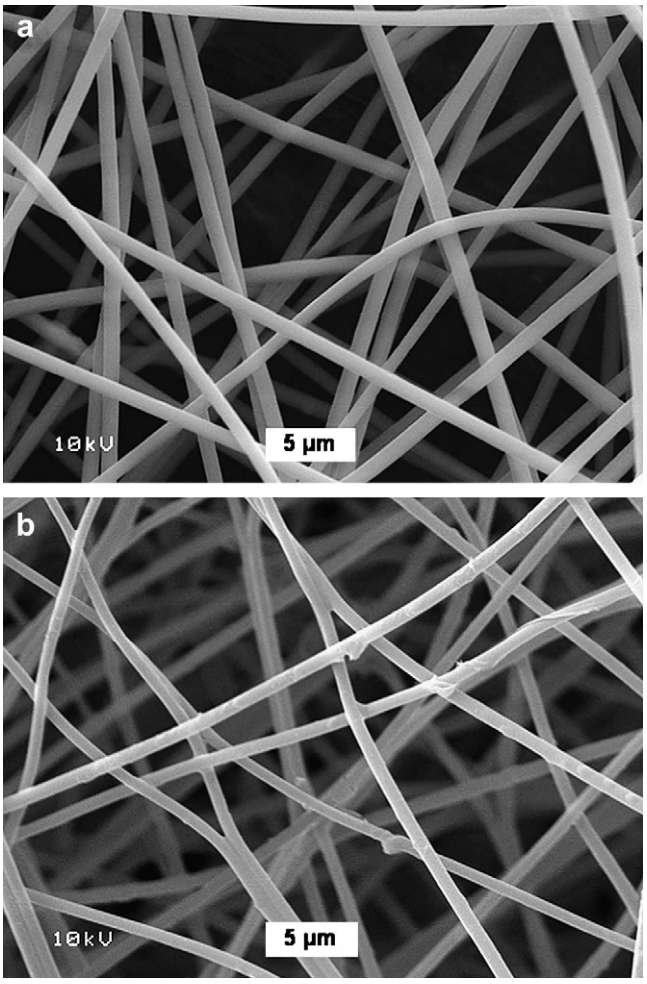

Fig. 3. SEM images of CA–CHX fibers: (a) as-spun fibers (fiber diameter: 950 ± 100 nm); (b) fibers after curing under saturated water vapor at 70 °C for 4 days.

3.2.2. Quantification of CHX content in the fibers

Table 3 shows the extent of CHX binding in the fibers determined by the UV–vis measurements.

As is seen, not all of the CHX was bound to the CA polymer matrix during the curing experiments. In the case of 7.0 wt% total CHX content in the fibers, almost all of the CHXs were coupled to the polymer matrix via TTE linkers. With increasing concentration of CHX in the fibers for a constant TTE concentration (1 wt% in spin solutions), the amount of unbound CHX increased dramatically, while the

Table 3
Extent of binding of CHX to the fibers

Total concentration of CHX in fibers[a] (wt%)	7.0	13.0	18.4	23.1
Bound CHX (wt%)	6.8 ± 0.1	5.5 ± 0.4	7.3 ± 0.7	8.1 ± 1.6
Unbound CHX (wt%)	0.2 ± 0.1	7.5 ± 0.4	11.1 ± 0.7	15.0 ± 1.6

[a] Derived from the solution compositions for electro spinning: 3.0 wt% CA, 0.2 wt% PEO, 1.0 wt% TTE and 0.3, 0.6, 0.9 or 1.2 wt% CHX.

concentration of bound CHX varied in a narrow range between 5 to 9 wt%. When the TTE concentration was increased from 1 to 2 wt% for fixed CHX concentrations in spin solutions, the resulting fibers possessed a similar concentration of bound CHX to that of the fibers electrospun from 1 wt% TTE solutions, suggesting that both CHX and TTE concentrations have a weak effect on the extent of CHX binding in these fibers. Thus, the concentration of bound CHX varies in a narrow range in these fibers while concentration of unbound CHX can be manipulated by controlling the concentration of CHX in the spin solutions.

3.2.3. Fiber characterization

The CA–CHX fibers were characterized by FTIR and Raman spectroscopies. FTIR and Raman spectra of fully washed CA–CHX fibers and cross-linked nonfunctional CA–TTE fibers are shown in Fig. 4.

The characteristic IR peaks of CHX observed between 1500 and 1650 cm^{-1} (C=N stretching and aromatic C=C bending vibrations, respectively) marked by a star (*) indicate the presence of CHX bound to the CA of the fibers. The same characteristic peaks were observed in the ATR-FTIR spectrum of CA–CHX fibers as well, indicating the presence of CHX on the fiber surface. Note the absence of these peaks when the CA–TTE fibers contained no CHX. In the Raman spectrum of the CA–CHX fibers, the characteristic CHX peak at 1610 cm^{-1}, as indicated by an arrow in Fig. 4, was observed. The peak is shifted 40 cm^{-1} to higher wavenumbers compared to that of pure CHX powders (1570 cm^{-1}), which could be attributed to the interaction of CHX with the polymer matrix in the fibers [44].

XPS was used to determine the surface composition of CA–CHX fibers; a typical XPS spectrum of fully washed CA–CHX fibers is shown in Fig. 5. The presence of titanium coupling agents on the surface layer was verified by the characteristic binding energy of Ti at 455 eV. The appearance of characteristic binding energies of N and Cl in the spectrum confirmed the presence of CHX bound within 10 nm of the surface of the fibers. The atomic ratio of Cl to C on the surface obtained from XPS measurements increased from 0.02 to 0.05,

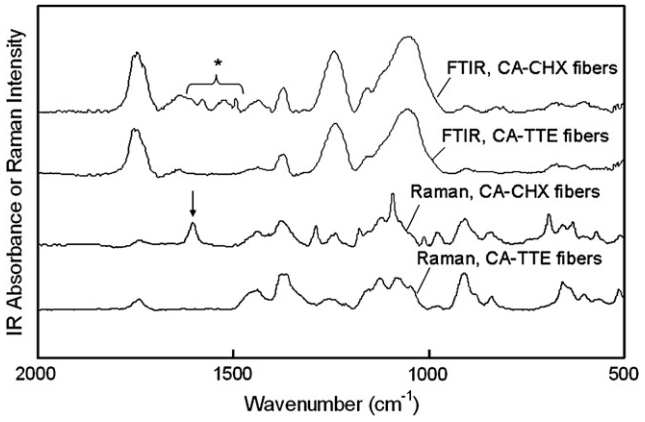

Fig. 4. FTIR and Raman spectra of fully washed CA–CHX fibers and nonfunctional CA–TTE fibers.

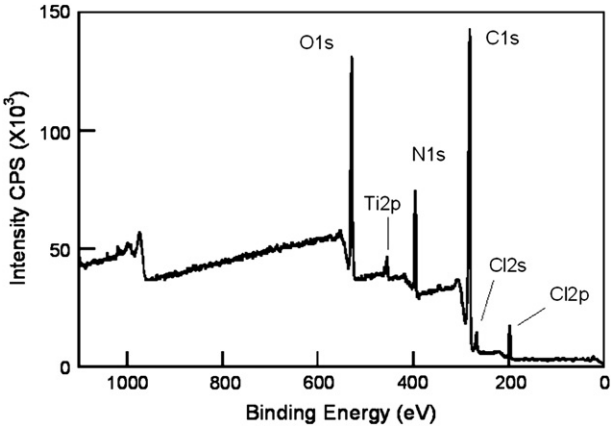

Fig. 5. XPS spectrum of fully washed CA–CHX fibers with 7.3 wt% of bound CHX.

while the atomic ratio of Cl to O increased from 0.07 to 0.30, as the concentration of CHX in the spin solutions was increased from 0.3 to 1.2 wt%. Both atomic ratios on the surface layer of these fibers were much greater than their bulk values (Cl/C: 0.01–0.02, Cl/O: 0.01–0.03) obtained by elemental analysis; this is indicative of enrichment of CHX on the surface of the fibers rather than in the core. CHX has been reported to be a surface-active compound and to form small aggregates in aqueous solution [45]. Such surface-active properties may promote the accumulation of CHX close to or on the surface of the jet during the electrospinning process.

3.2.4. Antibacterial activity

The release-killing capacity of unbound CHX in the fibers was evaluated by disk diffusion tests. The zone of inhibition (ZoI) was observed in all of the tested fiber samples, as indicated by the arrow shown in Fig. 6(a). In this test, unbound CHX in the fibers diffused out of the fibers, killing the bacteria nearby until the minimum inhibitory concentration of CHX (2–8 μg/ml for *E. coli* and 0.5–2 μg/ml for *S. epidermidis* [46]) was reached, below which bacteria can survive and proliferate. This resulted in the formation of a circular area where no bacterial colonies were observed. The size of the ZoI was measured from the edge of the circular fiber sample (22 mm in diameter) to the edge of the inhibition zone. Fig. 7(a) shows the ZoI determined by the disk diffusion tests against *E. coli* and *S. epidermidis* for four different fibers electrospun from four different CHX concentrations. Each datum point represents one type of fiber sample. The amount of CHX released per unit area was calculated from the weight of the circular fiber sample with a diameter of 22 mm (3–5 mg) and the concentration of unbound CHX in the fibers listed in Table 3. The curve shapes of ZoI vs. amount of CHX released per unit area (M) are very similar for *E. coli* and *S. epidermidis*. The ZoI increased significantly between 0 and 0.05 mg/cm^2 of CHX released, and then increased more gradually for amounts of the released CHX in excess of 0.05 mg/cm^2. Since this test method is based on the diffusion of unbound CHX, a simple one-dimensional diffusion model can describe the dependence of ZoI on the amount of released CHX from the fibers. That is,

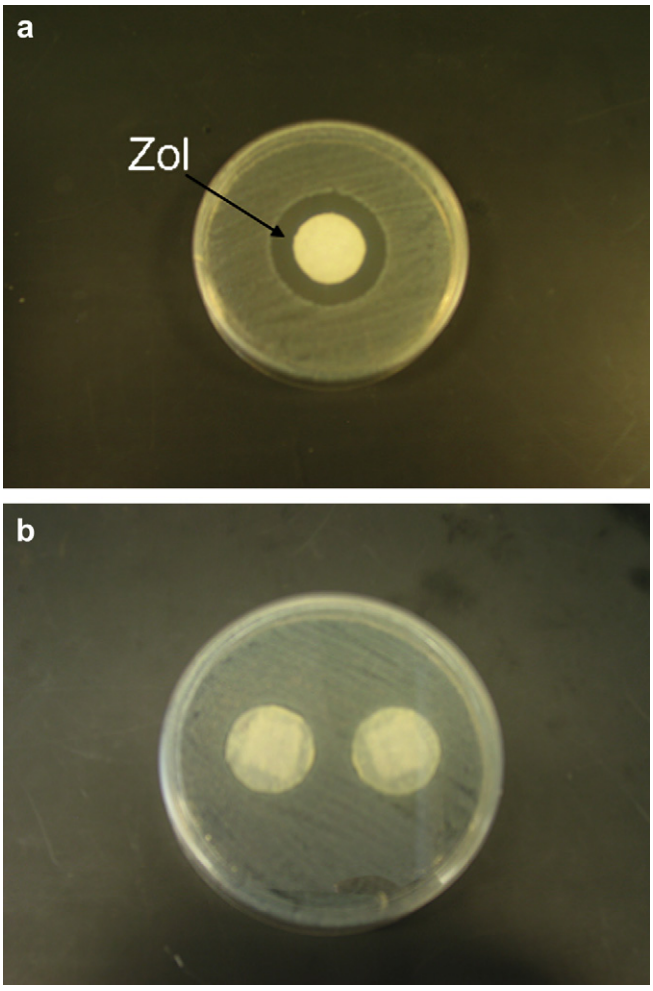

Fig. 6. Images of agar plates after disk diffusion tests (*E. coli*): (a) CA–CHX fibers without water treatment; (b) CA–CHX fibers completely washed out prior to test. (The two samples shown in (b) are identical.)

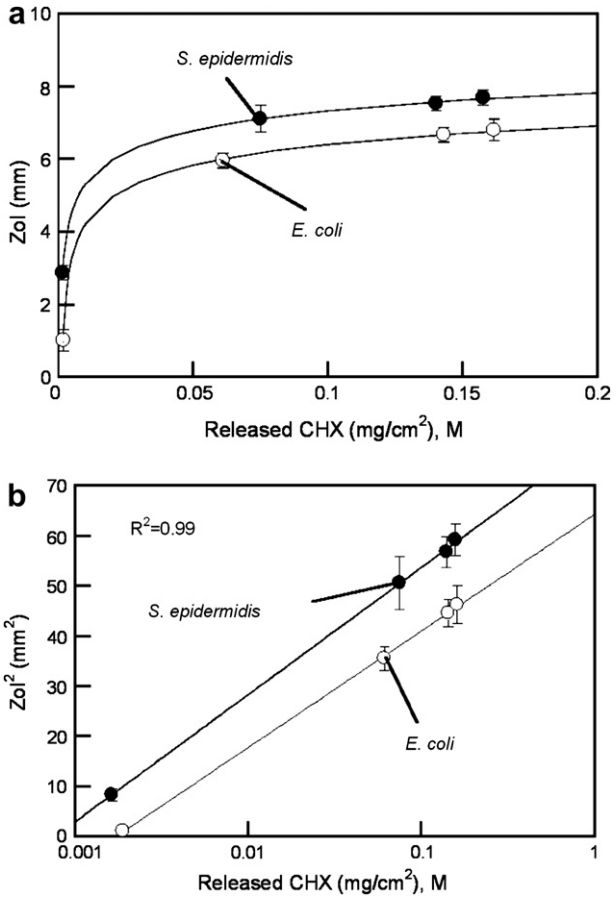

Fig. 7. Disk diffusion test results for CA–CHX fibers: (a) zone of inhibition (ZoI) vs. the amount of CHX released per unit area (M) of the fibers for *E. coli* and *S. epidermidis* (The solid curves were obtained by translating the corresponding linear regression lines of $(\mathrm{ZoI})^2$ vs. $\ln(M)$ in (b) into the ZoI vs. M plots.); (b) $(\mathrm{ZoI})^2$ vs. $\ln(M)$ for *E. coli* and *S. epidermidis*. (The solid lines are linear regression lines of $(\mathrm{ZoI})^2$ vs. $\ln(M)$.)

assuming radial diffusion of CHX the following relationship between M and ZoI can be derived [47,48]:

$$(\mathrm{ZoI})^2 = 4Dt\left(\ln\left(\frac{M}{M'}\right) + \ln C\right) \tag{6}$$

where M' is the critical inhibition amount of CHX released per unit area, below which bacteria can survive, D is the diffusion coefficient of CHX under the test conditions, t is the critical time for the formation of the inhibition zone (less than the incubation time), and C is a constant. Therefore, $\ln(M)$ should be linearly proportional to $(\mathrm{ZoI})^2$. The $(\mathrm{ZoI})^2$ vs. $\ln(M)$ dependencies were linear ($R^2 > 0.99$) for both *E. coli* and *S. epidermidis*, as shown in Fig. 7(b).

The contact-killing capacity of CHX bound to the fibers was tested via a modified ASTM E2149-01 procedure. Fig. 6(b) shows a typical image of the disk diffusion test results for these fully washed fibers. The absence of the ZoI confirmed the complete removal of free CHX. In the control experiment, the CA–TTE fibers without CHX were tested and did not show any killing of *E. coli* or *S. epidermidis*. Table 4 shows contact-killing bactericidal activity of the CHX fibers.

Since all four series of the tested fibers possessed a similar content of bound CHX, the fibers demonstrated similar contact-killing efficiencies, ranging from 94.2 to 99.9%. The XPS measurements indicate a trend toward increasing surface concentration of bound CHX with increasing CHX concentration in the spin solution, which could explain the slight increase in bactericidal efficiency (Table 4). Although the immobilization of CHX on/in the fibers may affect the CHX structure and the surrounding environment, our results indicate that the CHX bound on the CA fibers is still capable of killing the bacteria with as high as 3 log reduction or 99.9%

Table 4
Results of the contact-killing test by a modified ASTM E2149-01 procedure against *E. coli* and *S. epidermidis*

CHX concentration in spin solutions (wt%)	Bound CHX[a] (wt%)	Bactericidal efficiency (%)	
		E. coli	*S. epidermidis*
0.3	6.8	94.2	96.4
0.6	5.5	96.0	99.0
0.9	7.3	98.1	96.0
1.2	8.1	99.1	99.9

[a] Bulk value determined in Table 3.

bactericidal efficiency of the viable bacteria in 1 h. For comparison, identical fibers with the unbound CHX not washed out were tested using the modified ASTM E2149-01 procedure. The fibers with a total CHX content of 7.0 wt% exhibited a bactericidal efficiency similar to that of washed fibers with the same overall CHX content, because almost all of the CHX in the unwashed fibers was bound. However, the other three series of fibers with almost equal contents of the bound CHX ranging from 5 to 9 wt% and yet significant contents of unbound CHX (Table 3) showed more than 6 log reduction of viable bacteria due to the release of unbound CHX. Hence, the release of the unbound CHX in the fiber proximity seemed to lead to higher fiber efficiency.

3.3. Post-spin treatment of CA–PEO fibers

In addition to producing CHX-containing CA–CHX fibers via electrospinning of the blends of CA and CHX, we investigated a post-spin treatment process to prepare bactericidal fiber meshes. The post-spin treatment allowed us to attach the CHX onto the CA–PEO fibers via titanate linkers. The nonfunctional CA–PEO fiber meshes were immersed in diluted TTE solution and chlorhexidine digluconate solution, respectively, with each step followed by a curing process in the oven to covalently bind CHX onto the fibers. Fig. 8 shows SEM images of as-spun CA–PEO as well as post-spin treated fibers. The size of CA–PEO fibers is 920 ± 120 nm, which is similar to that of CA–CHX fibers electrospun from the blends (Fig. 3(a)). The fiber size was not affected by the post-spin treatment process (Fig. 8(b)), but formation of the titania clusters (*ca.* 150 nm in diameter) on the post-spin treated fibers was clearly discernible. The fiber meshes remained intact after the post-treatment while the porosity of the fiber mats may have changed during the treatment, as evidenced by a slight but visually observable shrinkage of the fiber meshes. Appearance of the characteristic peaks of CHX located at 1500–1650 cm^{-1} in ATR-FTIR spectra of the post-spin treated fibers confirmed the presence of CHX bound on the fibers after washing. Elemental analysis indicated that the amount of CHX attached onto the post-spin treated fibers was approximately 1–2 wt% of the total fiber weight. The antibacterial tests by the modified ASTM E2149-01 method showed that post-spin treated fibers (100 mg) were effective against *E. coli* with 99.6% reduction and *S. epidermidis* with 95.0% reduction of viable bacteria in 1 h. Compared with the results of the contact-killing tests of the CA–CHX fibers electrospun from polymer blends (Table 4), the post-spin treated fibers can achieve a similar antibacterial capacity with a much lower concentration of CHX attached to the fibers. We believe that repeated post-spin treatment of the fibers would increase the fiber loading for the bactericide, which would further enhance the bactericidal efficiency of the fibers.

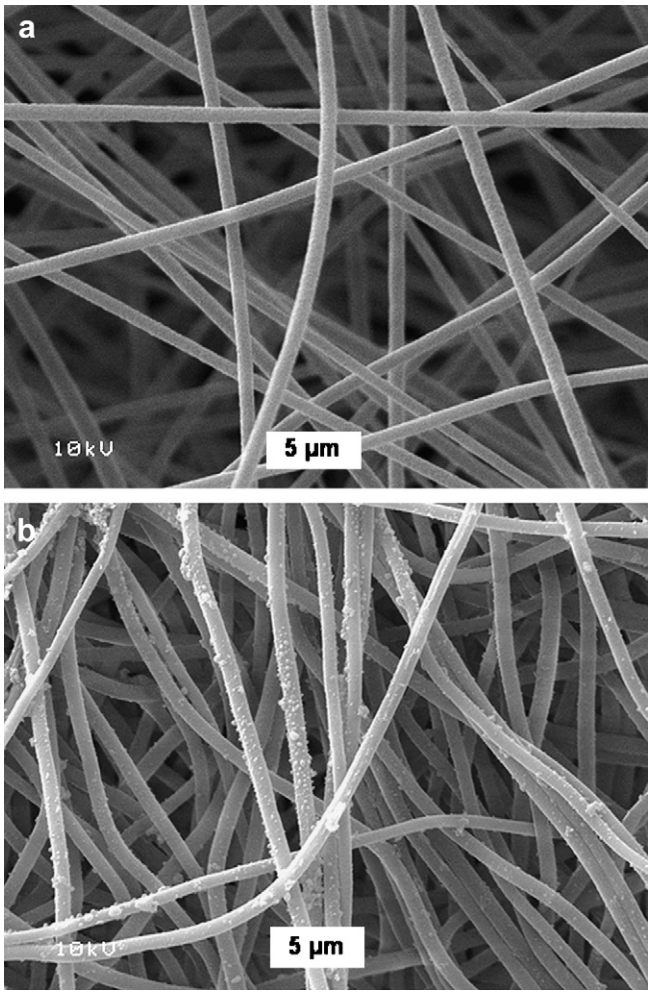

Fig. 8. SEM images of (a) as-spun nonfunctional CA–PEO fibers and (b) post-spin treated CA–PEO fibers with the attachment of CHX onto the fibers.

4. Conclusions

Bactericidal fiber meshes were successfully produced by the electrospinning of polymer blends containing the biocide, chlorhexidine (CHX). We show that the addition of a high molecular weight PEO to CA solutions significantly improves the elasticity of the CA solutions and facilitates the formation of fibers. A dimensionless *De* number, defined as the ratio of fluid relaxation time to instability growth time, was used to characterize the spinnability of the blends. It was found that uniform fibers were produced in the region of $De > 7$. The CA–CHX fibers demonstrated bactericidal capability not only through a gradual release of unbound CHX from the fibers but also via contact with CHX bound on the fibers. Antibacterial fiber mats were also obtained by post-spin treatment of CA–PEO fibers to immobilize CHX on the fibers via titanate linkers. The post-spin treated fibers achieved similar bactericidal efficiency compared to that of the CA–CHX fibers electrospun from the blends, even with a much lower CHX content. We surmise that a repeated post-spin treatment of the fiber could result in even higher CHX loading on the fiber surface and may further enhance the bactericidal properties of the fibers. We believe that the strategies presented in this work are not limited to incorporation of CHX only, but will also enable incorporation of a wide range of antibacterial agents such as antibiotics in/on the fibers.

Acknowledgements

This research was supported by the DuPont–MIT Alliance. The use of facilities of the Institute for Soldier Nanotechnologies and the Center for Materials Science and Engineering at MIT is acknowledged. The authors are grateful to Dr. Jian H. Yu and Dr. Pradipto Bhattacharjee for valuable discussions.

References

[1] Costerton JW, Stewart PS, Greenberg EP. Science 1999;284:1318.
[2] Lin J, Qiu S, Lewis K, Klibanov AM. Biotechnol Bioeng 2003;83:168.
[3] Sun Y, Sun G. J Appl Polym Sci 2003;88:1032.
[4] Danese PN. Chem Biol 2002;9:873.
[5] Ruggeri V, Francolini I, Donelli G, Piozzi A. J Biomed Mater Res A 2007;81A:287.
[6] Morris CE, Welch CM. Text Res J 1983;53:143.
[7] Dzenis Y. Science 2004;304:1917.
[8] Li D, Xia Y. Adv Mater 2004;16:1151.
[9] Fridrikh SV, Yu JH, Brenner MP, Rutledge GC. Phys Rev Lett 2003; 90:144502.
[10] Hohman MM, Shin M, Rutledge G, Brenner MP. Phys Fluids 2001; 13:2201.
[11] Hohman MM, Shin M, Rutledge G, Brenner MP. Phys Fluids 2001; 13:2221.
[12] Reneker DH, Yarin AL, Fong H, Koombhongse S. J Appl Phys 2000; 87:4531.
[13] Yarin AL, Koombhongse S, Reneker DH. J Appl Phys 2001;89:3018.
[14] Yarin AL, Koombhongse S, Reneker DH. J Appl Phys 2001;90:4836.
[15] Li D, Wang Y, Xia Y. Nano Lett 2003;3:1167.
[16] Wang M, Hsieh AJ, Rutledge GC. Polymer 2005;46:3407.
[17] Jin H-J, Chen J, Karageorgious V, Altman GH, Kaplan DL. Biomaterials 2004;25:1039.
[18] Wang X, Kim Y, Drew C, Ku B, Kumar J, Samuelson LA. Nano Lett 2004;4:331.
[19] Gibson P, Schreuder-Gibson H, Rivin D. Colloids Surf A 2001;187–188:469.
[20] Chen L, Bromberg L, Hatton TA, Rutledge GC. Polymer 2007;48:4675.
[21] Wang M, Singh H, Hatton TA, Rutledge GC. Polymer 2004;45:5505.
[22] Acatay K, Simsek E, Ow-Yang C, Menceloglu Y. Angew Chem Int Ed Engl 2004;43:5210.
[23] Ma ML, Hill RM, Lowery JL, Fridrikh SV, Rutledge GC. Langmuir 2005;21:5549.
[24] Schreuder-Gibson HL, Truong Q, Walker JE, Owens JR, Wander JD, Jones WE. MRS Bull 2003;28:574.
[25] Melaiye A, Sun Z, Hindi K, Milsted A, Ely D, Reneker DH, et al. J Am Chem Soc 2005;127:2285.
[26] Son WK, Youk JH, Lee TS, Park WH. Macromol Rapid Commun 2004; 25:1632.
[27] Ignatova M, Starbova K, Markova N, Manolova N, Rashkov I. Carbohydr Res 2006;341:2098.
[28] Ignatova M, Manolova N, Rashkov I. Eur Polym J 2007;43:1112.
[29] Odore R, Valle VC, Re G. Vet Res Commun 2000;24:229.
[30] Gjermo P. J Clin Periodontol 1974;1:143.
[31] Riggs PD, Braden M, Patel M. Biomaterials 2000;21:345.
[32] Yue IC, Poff J, Cortes ME, Sinisterra RD, Faris CB, Hildgen P, et al. Biomaterials 2004;25:3743.
[33] Yu JH, Fridrikh SV, Rutledge GC. Polymer 2006;47:4789.
[34] Anna SL, McKinley GH. J Rheol 2001;45:115.
[35] Rodd LE, Scott TP, Cooper-White JJ, McKinley GH. Appl Rheol 2005; 15:12.
[36] Shin YM, Hohman MM, Brenner MP, Rutledge GC. Polymer 2001; 42:9955.
[37] DuPont™ Tyzor® Organic Titanates General Brochure.
[38] Kramer J, Prud'homme RK, Wiltzius P. J Colloid Interface Sci 1987; 118:294.
[39] Menon N, Blum FD, Dharani LR. J Appl Polym Sci 1994;54:113.
[40] ASTM E2149-01 standard test method for determining the antimicrobial activity of immobilized antimicrobial agents under dynamic contact conditions. American Society for Testing and Materials: West Conshohocken, PA; 2004.
[41] Eggers J. Rev Mod Phys 1997;69:865.
[42] Goldin M, Yerushalmi J, Pfeffer R, Shinnar R. J Fluid Mech 1969; 38:689.
[43] Chang H-C, Demekhin EA, Kalaidin E. Phys Fluids 1999;11:1717.
[44] Jones DS, Brown AF, Woolfson D, Dennis AC, Matchett LJ, Bell SEJ. J Pharm Sci 2000;89:563.
[45] Sarmiento F, del Rio JM, Prieto G, Attwood D, Jones MN, Mosquera V. J Phys Chem 1995;99:17628.
[46] Buxbaum A, Kratzer C, Graninger W, Georgopoulos A. J Antimicrob Chemother 2006;58:193.
[47] Cooper KE. Analytical microbiology, vol. 1. New York: Academic Press; 1963 [chapter 1].
[48] Lee D, Cohen RE, Rubner MF. Langmuir 2005;21:9651.